OPEN

Characterization of Airflow Parameters in the Olfactory Fissure Zone Based on Fluid Mechanics Method

Feitong Jian, BS, Dielai Xie, MD,† and Shuo Wu, MD**

Objective: Airflow in the olfactory fissure region is a necessary condition for olfaction. However, due to the complex anatomy of the olfactory fissure, it is difficult to characterize the airflow in this region. At present, there are few studies on the airflow characteristics of the olfactory fissure. The aim of this study is to investigate the characteristics of objective indicators of airflow parameters in the olfactory fissure region, such as flow velocity, flow rate, pressure and flow ratio, from the perspective of biofluid mechanics.

Methods: In this study, the anatomical structure of the olfactory fissure zone was reconstructed in three dimensions using raw data from 32 healthy adults and 64 sinus computed tomography scans. To study the characteristics of airflow parameter variations in the olfactory fissure region in healthy adults, 10 cross-sectional sections were established in the olfactory fissure region using computational fluid dynamics after obtaining the airflow parameter values at different anatomical positions in the olfactory fissure region.

Results: The average flow rate of the ten cross-sections in the olfactory fissure zone was 19.22 ± 9.74 mL/s, the average flow velocity was 0.51 ± 0.21 m/s, the average flow percentage was $5.45\% \pm 2.52\%$, and the average pressure was -13.35 ± 6.74 Pa. The percentile method was used to determine the range of reference values for P90: average flow rate of 0.02–35.87 mL/s, average flow velocity of 0.24–0.94 m/s, average flow percentage of 1.57%–9.93%, and average pressure of −30.4–4.42 Pa. Among the ten cross-sectional systems of the olfactory fissure, the median of Plane3N-Plane8N is more stable and representative. In the olfactory fissure system, the corresponding anatomical position of Plane3N-Plane8N was in the posterior region of the olfactory fissure, mainly at the junction of the anterior, middle 1/3 to the posterior middle turbinate, which was consistent with the main distribution area of the olfactory mucosa.

Conclusion: This study shows that the application of computational fluid dynamic can rapidly achieve the characterization of airflow parameters in the olfactory fissure. The airflow through the olfactory fissure in healthy adults accounted for no more than 10% of the total flow volume of the nasal cavity. The airflow parameters in the anterior region of the olfactory fissure fluctuated significantly, while those flowing through the posterior region of the olfactory fissure were more stable. This could be due to the anterior section of the middle turbinate truncating the restriction of airflow into the olfactory fissure.

Key Words: airflow parameter, computational fluid dynamics, olfactory fissure

(*J Craniofac Surg* 2023;34: 532–535)

The incidence of olfactory dysfunction is as high as 67.0% because of nasal diseases.[1] The olfactory function of these patients' original structurally poor nasal cavity can be restored to varying degrees after endoscopic surgery. This is closely related to removing conductive olfactory factors caused by poor nasal anatomy and restoring airflow in the olfactory fissure. Multiple studies have demonstrated that the airflow in the olfactory fissure is closely related to the sense of smell.[2,3] The olfactory fissure is a deep, narrow, irregular fissure at the top of the nasal cavity. Due to its complex anatomy, it is difficult to be reconstructed realistically and accurately. Therefore, it has become a challenge to obtain the airflow parameters of the olfactory fissure. There has been little research on the peculiarities of the airflow parameters of the olfactory fissure region since they are difficult to collect. Kelly et al[4] developed various models of the entire nasal cavity and discussed the influence of the airflow characteristics of the olfactory fissure region by replacing the physiological and pathological changes of the nasal airflow with those of the olfactory fissure region. Nowadays, many studies are still limited to the effect of nasal airflow changes on nasal physiology, while studies on the airflow characteristics of the olfactory fissure region are still lacking.[5,6]

Computational fluid dynamics (CFDs) is a biomechanical method that has been rapidly developed in recent years to study nasal airflow.[7–9] Croce and colleagues and Kimi and colleagues have studied the overall nasal flow field in healthy individuals using the CDF technique. Nomura et al[10] used this technique to

From the Departments of *ENT; and †Radiology, The 3rd Affiliated Hospital, Sun Yat-Sen University, Guangzhou, People's Republic of China.

Received June 17, 2022.

Accepted for publication August 24, 2022.

Address correspondence and reprint requests to Shuo Wu, Department of ENT, The 3rd Affiliated Hospital, Sun Yat-Sen University, No. 600 Tianhe, Road, Tianhe District, Guangzhou 510630, People's Republic of China; E-mail: wush68@sysu.edu.cn

The authors report no conflicts of interest.

Supplemental Digital Content is available for this article. Direct URL citations appear in the printed text and are provided in the HTML and PDF versions of this article on the journal's website, www.jcraniofacialsurgery.com.

ISSN: 1049-2275

DOI: 10.1097/SCS.0000000000009075

analyze the airflow field of the nasal cavity before and after surgery for different pathological conditions to evaluate the effect. Alam et al[11] used the CFD technique to analyze the changes in the nasal airflow field and the effect on olfactory function after virtual middle turbinate resection and found that nasal resistance decreased, and olfactory flux increased after middle turbinate resection. They suggested that individual differences in the anatomy of the olfactory fissure region and changes in airflow parameters may be related to olfactory function.

To investigate the airflow characteristics of the olfactory fissure, this study conducted a 3D modeling of the nasal olfactory fissure based on sinus computed tomography (CT) imaging data, obtained various parameters such as airflow, velocity, pressure, and flow ratio in the olfactory fissure by fluid mechanics analysis, and established a cross-sectional system to analyze the airflow characteristics at different positions in the olfactory fissure.

METHODS

Study Participants

All eligible healthy adults were screened for clinical ENT examinations, spiral CT of the sinuses, nasal endoscopy, nasal sound, and nasal obstruction examinations, and Sniffin' Sticks test. The following selection criteria were used for volunteers: a visual analog scale score of 0 for nasal symptoms; a LUND-Mackay score of 0 for sinus CT; no history of chronic nasal disease; no history of head trauma; no history of nasal medication use within the past three months; a composite threshold-discrimination-identification score of at least 30 on the Sniffin' Sticks test.

All selected volunteers signed an informed consent form. This paper was approved by the Clinical Medical Research Ethics Committee of the Third Affiliated Hospital of Sun Yat-sen University [Batch No. 02-079-01 (2020)].

Study Procedures

Three-dimensional Modeling of the Nasal Olfactory Fissure

The selected volunteers underwent sinus CT at the Third Affiliated Hospital of Sun Yat-sen University. The scanning equipment was a multirow spiral CT produced by Philips with a thickness of 0.5 mm. We then obtained the file in DICOM format, extracted the pixels using MIMICS software, created a 3D point cloud data in 3D view (Fig. 1A), and used Calculate 3D from masks of MIMICS software to generate a 3D model from the edited masks (Fig. 1B). The nasal cavity model was analyzed using the Mesh Doctor function in Geomagic Studio (Fig. 1C), and the accuracy of the model was verified by analyzing the overall nasal flow field using the 3D solid geometry model of the nasal cavity generated by model software (Fig. 1D). The olfactory fissure region was extracted from different sections along the coronal direction using the cross-sectional function of model software. Then the smallest polygon for enveloping (Fig. 1E) and the coordinate information of the polygon vertices were extracted by the measurement tool, and the drawn polygon vertices were extracted by the measurement tool and saved as coordinates (Fig. 1F). Finally, the 3D modeling of the nasal olfactory cleft region was realized, laying the foundation for the following flow field mechanics analysis. The process is shown in Figure 1.

Meshing of the Nasal Cavity Model

The meshing of the nasal cavity model is an important step in fluid dynamics analysis. The quality of mesh delineation directly affects the accuracy of calculation results. In this paper, ANSYS ICEM CFD software was used for meshing, and the 3D model was divided into 3 parts: inlet, outlet, and wall. Each nose was different, so the specific parameters were different when dividing the mesh. Regarding the independence of the grid, when we studied the first nose model, we had already conducted experiments and determined the approximate magnitude of the grid. The mesh of each nose model was about the same order of magnitude. Therefore, uniformity in the order of magnitude can guarantee the grid independence. Take volunteer No. 1 for example, so the number of mesh nodes was 418069, the number of elements was 2473513, the tetrahedral mesh was 2246637, and the triangular mesh was 171881. Finally, the nasal cavity model with nearly 2.5 million meshes was obtained to ensure the accuracy of the calculation results.

Setting of Boundary Conditions

According to the actual situation of breathing, we set the boundary conditions of the nasal cavity. The boundary condition of the outlet (inferior nasopharynx) was set as a flow boundary condition with a size of 360 mL/s. The inlet was a pressure inlet with a free boundary and its pressure was one standard atmosphere. The wall surface was nonsliding, and the roughness was set at 0.5 mm.[12]

Establishment of Cross-Sectional Sections and Analysis of the Flow Field in the Olfactory Fissure

In this paper, the airflow fields of the nasal cavity and paranasal sinuses were simulated based on the ANSYS Workbench platform.[11] The nasal airflow is an incompressible Newtonian fluid and the governing equations for nasal breathing are the continuity equation and the N-S equation. During the simulations, the standard K-ε turbulence model was chosen. The fluid medium was t air with a density of 1.25 kg/m^3 and a viscosity of 1.7894×10^{-5} Ns/m^2. Using Fluent as a solver to simulate nasal fluid dynamics, various airflow parameters could be obtained for any cut-off point of the nasal cavity and sinuses.

In order to reflect the variation of airflow parameters at different locations in the olfactory fissure region, a cross-sectional section (Plane 1N-10N) was established in this paper.[8] The anterior edge of the middle turbinate and the corresponding surface of the nasal septum were used as the entrance to the olfactory fissure, and the narrow, long, and irregular olfactory fissure region formed by the medial surfaces of the middle and superior turbinates, and the corresponding nasal septum was divided equally into 10 parts along the coronal direction.[9] The interface data was extracted by the section function of model software to analyze the different positions of the entire olfactory fissure. Finally, the airflow, velocity, pressure, and flow ratio data were obtained for 10 sections representing different positions of the olfactory fissure within each nasal cavity. Plane 1–3N sections correspond to the junction area between the middle turbinate and the middle third of the middle turbinate, the anterior olfactory fissure area. Plane 4–10N sections correspond to the anterior one-third of the middle turbinate junction with the anterior wall of the sphenoid sinus, which is the posterior olfactory fissure zone. The analysis of the airflow parameters of the 10 cross-sectional sections in the olfactory fissure region is shown in Figure 2.

All 32 volunteers with 64 nasal cavities were modeled based on CT data of the sinuses using the above method. Then the

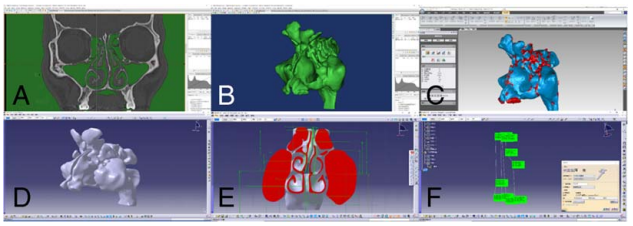

FIGURE 1. Three-dimensional model establishment process.

airflow through the olfactory fissure of the nasal cavity was analyzed according to a predesigned cross-sectional system. The mean velocity, pressure, and flow rate of the airflow in 10 cross-sections of each nasal cavity were obtained, as well as the proportion of flow through the olfactory fissure. Based on the cross-sectional system, the nasal olfactory fissure zones were divided for each case, and the mean flow rate, pressure, velocity, and flow ratio were calculated for each cross-section. A total of 2560 parameter values were obtained.

RESULTS

Using the CFDs analysis method, based on the CT model of the nasal cavity and sinuses in the first step, a total of 64 cases of 32 volunteers were analyzed according to the predesigned cross-sectional system. Ten cross-sectional systems were analyzed by statistically analyzing the average velocity of airflow movement, pressure, and flow rate in the olfactory fissure zone of airflow. The average flow through the 10 cross-section systems in the olfactory fissure zone was 19.22 ± 9.74 mL/s. The average flow velocity was 0.51 ± 0.21 m/s. The average flow ratio was 5.45% ± 2.52%. The average pressure was –13.35 ± 6.74 Pa. The percentile method was used to determine the p5–p95 range of airflow parameters for all 4 groups of healthy volunteers. The average flow rate was 0.02–35.87 mL/s. The average flow rate was 0.24–0.94 m/s. The average flow ratio was 1.57%–9.93%. The average pressure was −30.4–4.42 Pa, as shown in Supplemental Table 1, Supplemental Digital Content 1, http://links.lww.com/SCS/E611.

Statistical analysis of fluid characteristic parameters in olfactory fissure zone

Based on the 10 predesigned cross-sectional sections in the olfactory fissure zone, the airflow parameter data of each section was compared with the median data. The median value of Plane 3N–Plane 8N in the cross-sectional system was more stable, and the airflow was also more stable (Fig. 3). In the olfactory fissure, the anatomical location of Plane 3N–Plane 8N was mainly concentrated at the junction of the anterior one-third of the middle turbinate, starting at the posterior end of the superior turbinate, that is, the posterior region of the olfactory fissure, which was consistent with the main distribution area of the olfactory mucosa.

DISCUSSION

This paper started with digital 3D modeling of the nasal cavity and paranasal sinuses using improved multisoftware serialization and optimization to achieve rapid modeling of the nasal olfactory fissure region. We investigated the variation of airflow parameters in 64 cases of nasal olfactory fissure in 32 healthy adults with normal olfaction. Due to the different anatomical structures of the nasal cavity and the olfactory fissure zone, we found that the values of airflow, velocity, pressure, and flow ratio in the olfactory fissure zone varied significantly, and the trends of airflow parameters in different positions were basically

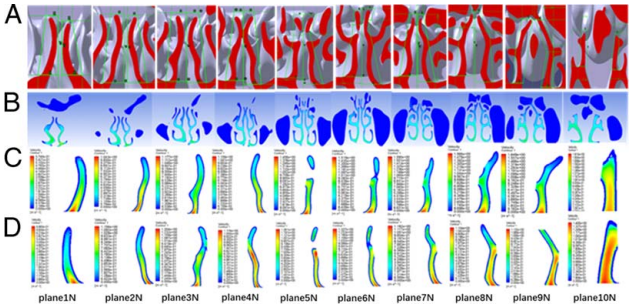

FIGURE 2. Flowing parameters of the 1–10 cross-sectional section. A, Imaging position corresponding to each section. B, Airflow velocity at the overall nasal cavity of each section. C, Airflow velocity at the right olfactory fissure position of each section. D, Airflow velocity at the left olfactory fissure position of each section.

the same. The airflow through the olfactory fissure zone accounted for <10% of the entire nasal airflow, which is consistent with the studies of Cherobin et al[13] and Nomura et al[10] on the variation of airflow throughout the nasal cavity. There are limited studies on the other 3 airflow parameters that pass through the olfactory fissure zone in the literature. In 64 cases, the average velocity P90 in the olfactory fissure zone of the nasal cavity was 0.24–0.94 m/s, less than one-fifth of the maximum velocity of 4–5 m/s in the nasal cavity.[10] We analyzed the phenomenon of significant slowing of airflow velocity into the olfactory fissure. The physiological significance may be that it facilitates the deposition of olfactory particles into the airflow, increasing the intensity of stimulation of the olfactory mucosal epithelium and ultimately affecting the olfactory function.

In this study, when exploring the changes in airflow parameters at different locations of the olfactory fissure zone through 10 cross-sectional systems, we found that the 4 airflow parameters at the position of Plane 1N–Plane 3N fluctuated, while the airflow parameters at the position of Plane 3N–Plane 10N were relatively stable. The anterior one-third of the middle turbinate corresponding to the threshold airflow of the olfactory fissure zone had a large variation. The anterior middle turbinate has a limiting effect on the airflow into the olfactory fissure threshold so that the airflow into the olfactory fissure threshold is maintained in a stable range, while the posterior region of the olfactory fissure is the main distribution area of the olfactory mucosa, so the stability of the airflow in the posterior region of the olfactory fissure may have an important effect on the olfactory function. In their studies of the effect of middle turbinate resection on olfaction, Wexler et al[9] and Alam et al[11] concluded that middle turbinectomy increased nasal airflow and

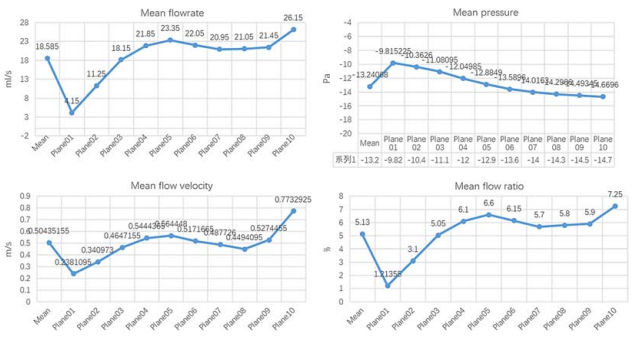

FIGURE 3. The range of statistical values of fluid characteristic parameters in the olfactory fissure zone.

facilitated the improvement of olfaction. Our study found that the anterior aspect of the middle turbinate may play an important role in maintaining the stability of airflow in the olfactory fissure. Although removal of the anterior aspect of the middle turbinate may increase the airflow into the olfactory fissure, it may affect the stability of the airflow in the olfactory fissure region and adversely affect the olfactory function.

CONCLUSION

In this paper, the characteristics of the airflow parameters in the olfactory fissure area of healthy adults are discussed from the flow field characteristics of the nasal cavity. The P90 reference range of airflow parameters in the olfactory cleft area of healthy adults was obtained by hydrodynamic analysis. However, due to the limited number of study cases, the range of airflow parameters in the olfactory fissure region of healthy adults still needs to be determined by many study cases in future studies. This study investigated the trends of airflow velocity, flow rate, flow ratio, and pressure at different locations in the olfactory fissure region, which laid the foundation for future studies on the relationship between airflow characteristics and olfactory function in the olfactory fissure area.

REFERENCES

1. Kohli P, Naik AN, Harruff EE, et al. The Prevalence of olfactory dysfunction in chronic rhinosinusitis. *Laryngoscope* 2017;127:309–320
2. Aydoğdu I, Atar Y, Aydoğdu Z, et al. Comparison of olfactory function and quality of life with different surgical techniques for nasal septum deviation. *Craniofac Surg* 2019;30:433–436
3. Vandenhende-Szymanski C, Hochet B, Chevalier D, et al Olfactory cleft opacity and CT score are predictive factors of smell recovery after surgery in nasal polyposis. *Rhinology* 2015;53:29–34
4. Kelly JT, Prasad AK, Wexler AS. Detailed flow patterns in the nasal cavity. *Appl Physiol* 2000;89:323–337
5. Subramaniam RP, Richardson RB, Morgan KT, et al. Computational fluid dynamics simulations of inspiratory airflow in the human nose and nasopharynx. *Inhal Toxicol* 1998;10:91–120
6. Hahn I, Scherer PW, Mozell MM. Velocity profiles measured for airflow througha large-scale model of the human nasal cavity. *J Appl Physiol* 1993;75:2273–2277
7. Lindem Ann J, Keck T, Wiesmiller K, et al. Nasal air temperature and air flow during respiration in numerical simulation based on multislice computed tomography scan. *Am J Rhino l* 2006;20:219–223
8. Zhao K, Dalton P, Yang GC, et al. Numerical modeling of turbulent and lamina r air flow and odorant transport during sniffing in the human and rat nose. *Chem Senses* 2006;1:107–118
9. Wexler D, Segal R, Kimbell J. Aero dynamic effects of inferior turbinate reduction. *Arch Otolaryngol Head Neck Surg* 2005;131:1102–1110
10. Nomura T, Ushio M, Kondo K, et al. Effects of nasal septum perforation repair surgery on three-dimensional airflow: an evaluation using computational fluid dynamics. *Eur Arch Otorhinolaryngol* 2015;272:3327–3333
11. Alam S, Li C, Bradburn KH, et al. Impact of middle turbinectomy on airflow to the olfactory cleft: a computational fluid dynamics study. *Am J Rhinol Allergy* 2019;33:263–268
12. de Gabory L, Reville N, Baux Y, et al. Numerical simulation of two consecutive nasal respiratory cycles: toward a better understanding of nasal physiology. *Intl Forum Allergy Rhinol* 2018;8:676–685
13. Cherobin GB, Voegels RL, Gebrim EMMS, et al. Sensitivity of nasal airflow variables computed via computational fluid dynamics to the computed tomography segmentation threshold. *PLoS One* 2018;13:e0207178

